Available online at www.sciencedirect.com
SCIENCE DIRECT®
Computers and Structures 82 (2004) 301–314
Computers & Structures
www.elsevier.com/locate/compstruc

Nonlinear reduced models for beam damage detection using data on moving oscillator–beam interactions

L. Majumder, C.S. Manohar *

Department of Civil Engineering, Indian Institute of Science, Bangalore 560012, India

Received 8 May 2002; accepted 19 August 2003

Abstract

The problem of detecting local and/or distributed loss of stiffness in beam structures using vibration data generated by passage of a moving oscillator is considered. A time domain structural damage detection scheme, within finite element modeling framework, that takes into account time varying structural matrices, structural nonlinearities and spatial incompleteness of measured data, is developed. The damage parameters associated with changes in structural stiffness are shown to be governed by a set of overdetermined nonlinear equations which are solved iteratively. Illustrative examples on a geometrically nonlinear Euler–Bernoulli beam carrying a moving single degree of freedom oscillator are provided.

Keywords: Damage detection; Time domain analysis; Model reduction

1. Introduction

Research into the use of vibration data in damage detection is presently attracting wide attention. Most of the currently available methods aim to relate the changes in natural frequencies, modeshapes, or frequency response functions to the occurrence of structural damage. Thus, these methods are developed essentially as applications of the traditional experimental modal analysis procedures [1–3]. The methods developed in the context of finite element (FE) model updating also serve as valuable tools in damage detection procedures [4,5]. Thus, the method of inverse eigensensitivity and response function method form powerful tools for element level identification of structural damages. One of the questions that is attracting significant research attention is related to the use of structural response to operational dynamic loads in damage detection procedures: see, for example, the papers by Wang and Haldar [6] and Hermans and Auweraer [7]. In fact, the review paper by Doebling et al. [8] identifies this class of problems as requiring further research attention.

In the context of civil structural health monitoring, the use of vibration data in damage detection has been discussed by a few authors. Thus, Mazurek and Wolf [9] have studied theoretically and experimentally a two span aluminum plate girder under the action of moving loads with view to identify structural deterioration using vibration signature analysis. Hearn and Testa [10] conducted studies on fatigue damaged welded steel building frames and wire ropes and studied shifts in frequency spectra caused due to damage. Yao et al. [11] considered the redistribution of energy upon the occurrence of damage and discussed the concept of strain modeshapes in characterizing the local structural damage. Alampalli and Fu [12], Alampalli [13], Allampalli et al. [14] and Alampalli and Cioara [15] address the problem of modal testing and analysis of structures under operational loads. The use of dynamic response as an inspection tool to assess bearing conditions and girder cracking in

* Corresponding author. Tel.: +91-80-309-2667; fax: +91-80-360-0404.
E-mail address: manohar@civil.iisc.ernet.in (C.S. Manohar).

0045-7949/$ - see front matter © 2003 Elsevier Ltd. All rights reserved.
doi:10.1016/j.compstruc.2003.08.007

concrete bridge structures has been investigated by Casas and Aparicio [16]. Issues related to the mismatch between measured and modeled degrees of freedom in large scale building frames have been examined by Koh et al. [17] in the context of damage detection problems. Liu [18] has examined the identifiability of inverse problems and influence of input errors on identification process in the context of damage detection in truss structures. The study by Salawu and Williams [19] describes full-scale vibration tests conducted before and after structural repairs on a multi-span reinforced concrete highway bridge. Wahab and Roeck [20] describe the results of field vibration tests on three concrete bridges with a view to correlate FE models with test results. The use of residual force vector and a sensitivity analysis has been made by Kosmatka and Ricles [21] in their study on a 10-bay space truss.

Recently, the present authors have developed a time domain formulation to detect beam damages using data emanating from linear beam–oscillator dynamic interactions [22]. This study has been conducted as a prelude to the study of damage detection in bridge structures using vibration data generated by the passage of a test vehicle. Thus, to a first approximation, the bridge structure is idealized as a simply supported beam and the vehicle as a moving single degree of freedom (sdof) oscillator with sprung and unsprung masses. The governing equations of motion in this case are known to constitute a set of differential equations with time varying coefficients. Thus, data coming from such a system are not useful in damage detection if conventional frequency/modal domain approaches are to be employed. Consequently, the present authors employed a time domain formulation to detect damages. The present study aims to extend the capabilities of this formulation to include the possibility of the damaged beam structure undergoing nonlinear vibrations. This we believe is important, especially, since the dynamical behavior of nonlinear systems many a times could be significantly different from that predicted from a simplified linear model. It may be noted in this context that nonlinearity in moving oscillator structure interaction can arise because of one or more of the following reasons:

- nonlinear strain–displacement relation in beam and/or the oscillator structure;
- nonlinear stress–strain relation and/or presence of nonlinear dissipation mechanism in the oscillator and/or beam structure;
- the possibility of oscillator losing contact with the beam structure as it traverses the beam. The propensity for such a separation to occur is enhanced, especially, if oscillator accelerates while on the beam and the beam deck is significantly uneven;
- presence of cracks, mainly in the beam structure, which open and close during vibrations.

The studies by Hino et al. [23], Yoshimura et al. [24] and Lee [25] are representative of investigations into computational modeling of nonlinear oscillator-structure interaction problems. In the present study, we consider the problem of damage detection in beam structures using vibration data that originate from nonlinear oscillator interactions. The structural and motion characteristics of the oscillator are assumed to be known. This would mean that the oscillator that is being used is deemed to be a "test" oscillator whose characteristics are well understood. We limit our attention in this study to only one source of nonlinearity, namely, the presence of nonlinear strain–displacement relations in the beam structures. Issues arising out of spatial incompleteness of measured data are also discussed. Illustrative examples involving beam structure modeled as a Euler–Bernoulli beam and the oscillator as a moving sdof oscillator are presented.

2. Finite element model for nonlinear VSI

Fig. 1 shows an idealized model for a beam–oscillator system. Here the beam structure is modeled as a single span Euler–Bernoulli beam and the oscillator is modeled as a moving sdof oscillator with a sprung and an unsprung mass. The beam, in its undamaged state, is taken to be simply supported and is allowed to have spatially varying flexural rigidity. The types of damages that are considered in this study include local and/or distributed loss of stiffness in the beam structure and the possibility of the bearings becoming partially immobile. In a practical structure, in case the bearings become immobile due to inadequate maintenance, it would then offer unanticipated resistance to rotations at the support, thereby leading to unwanted bending stress near the supports. In the present study, the effect of partially immobile bearings is idealized by the emergence of a rotary spring at the ends as shown in Fig. 1. For the beam, in its undamaged state, the value of the rotary springs at the ends would clearly be zero. The oscillator is assumed to travel with a velocity v_0 and an accelera-

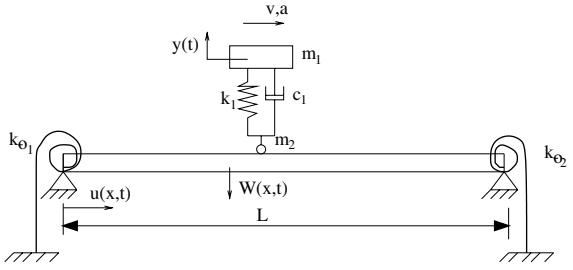

Fig. 1. Beam–oscillator system with partially immobile bearings.

tion a_0. The oscillator enters the beam at $t = 0$ and exits the beam at $t = t_f$. At $t = 0$, the beam is assumed to be at rest and the beam deck is taken to be free from any surface irregularities. The strain–displacement relationships for the beam structure are assumed to be nonlinear while the stress–strain relations are taken to be linear. Furthermore, the oscillator is assumed to be in contact with the beam deck at all times while it traverses the beam. Under these assumptions, the equation of motion for the beam–oscillator system, valid for the time interval $0 \leqslant t \leqslant t_f$, can be shown to be given by [23]

$$m_1\ddot{y} + c_1\left[\dot{y} - \frac{D}{Dt}\{w(x,t)\}\right] + k_1\{y - w(x,t)\} = 0,$$
$$\text{with } x(t) = vt + \frac{1}{2}at^2, \tag{1}$$

$$m(x)\frac{\partial^2 u(x,t)}{\partial t^2} + c_a\frac{\partial u(x,t)}{\partial t} = \frac{\partial}{\partial x}\left\{\mathrm{AE}(x)\left[\left(\frac{\partial u(x,t)}{\partial x}\right) + \frac{1}{2}\left(\frac{\partial w(x,t)}{\partial x}\right)^2\right]\right\}, \tag{2}$$

$$\frac{\partial^2}{\partial x^2}\left[\mathrm{EI}(x)\frac{\partial^2 w(x,t)}{\partial x^2}\right] - \frac{\partial}{\partial x}\left[\mathrm{AE}(x)\left\{\left(\frac{\partial u(x,t)}{\partial x}\right) + \frac{1}{2}\left(\frac{\partial w(x,t)}{\partial x}\right)^2\right\}\right]\frac{\partial w(x,t)}{\partial x} + c\frac{\partial w(x,t)}{\partial t} + m(x)\frac{\partial^2 w(x,t)}{\partial t^2} = f(x,t)\delta\left(x - v_0 t - \frac{1}{2}a_0 t^2\right), \tag{3}$$

$$f(x,t) = (m_1 + m_2)g + k_1[y(t) - w(x,t)] + c_1\left[\dot{y}(t) - \frac{D}{Dt}\{w(x,t)\}\right] - m_2\frac{D^2}{Dt^2}\{w(x,t)\}. \tag{4}$$

In these equations m_1 = oscillator sprung mass, m_2 = oscillator unsprung mass, c_1 = damping coefficient for the oscillator suspension, k_1 = spring stiffness of the oscillator suspension, g = acceleration due to gravity, x = spatial coordinate, t = time, $y(t)$ = vertical displacement of the oscillator sprung mass, $w(x,t)$ = transverse displacement of the beam, $u(x,t)$ = axial displacement of the beam, $\mathrm{AE}(x)$ = axial rigidity of the beam, c_a = damping coefficient in axial motion, $m(x)$ = mass per unit length of the beam, $\mathrm{EI}(x)$ = flexural rigidity of the beam, c = damping coefficient in transverse motion, and $\delta(\cdot)$ = Dirac's delta function. The total derivative D/Dt appearing in the above equations takes into account the Coriolis effect arising from the rolling of the oscillator mass on the deflected profile of the beam. The boundary conditions appropriate for the system under consideration are

$$\begin{aligned} &u(0,t) = 0, \quad w(0,t) = 0,\\ &\left[\mathrm{EI}(0)\frac{\partial^2 w(0,t)}{\partial x^2}\right] + k_{\theta 1}\frac{\partial w(0,t)}{\partial x} = 0,\\ &u(L,t) = 0; \quad w(L,t) = 0,\\ &\left[\mathrm{EI}(L)\frac{\partial^2 w(L,t)}{\partial x^2}\right] - k_{\theta 2}\frac{\partial w(L,t)}{\partial x} = 0. \end{aligned} \tag{5}$$

In these equations L = beam span, and $k_{\theta 1}$ and $k_{\theta 2}$ = rotary stiffness at the beam ends that develop due to bearings becoming immobile. After the oscillator exits the beam, that is, for $t \geqslant t_f$, the governing equations for the beam are given by Eqs. (2) and (3) with $f(x,t) = 0$. Furthermore, the initial conditions, at $t = t_f$, for these equations are obtained by solutions of Eqs. (1)–(3) at $t = t_f$.

To obtain a FE model, commensurate with the above equations of motion, the beam is divided into n_e number of elements, and, in the kth element, the displacement fields $u(x,t)$ and $w(x,t)$ are represented using cubic and quadratic polynomials, respectively [26] (see, Fig. 3). Subsequently, using Galerkin's finite element formulation, the governing equation of motion in the discretized form for the beam–oscillator system, for $0 < t \leqslant t_f$, can be shown to be of the form

$$\begin{pmatrix} \mathscr{M}_{bb}(t) & \{0\} & \{0\} \\ \{0\} & \mathscr{M}_{aa} & \{0\} \\ \{0\} & \{0\} & m_1 \end{pmatrix}\begin{Bmatrix} \{\ddot{d}_b\} \\ \{\ddot{d}_a\} \\ \ddot{y} \end{Bmatrix} + \begin{pmatrix} \mathscr{C}_{bb}(t) & \{0\} & \mathscr{C}_{by}(t) \\ \{0\} & \mathscr{C}_{aa} & \{0\} \\ \mathscr{C}_{yb}(t) & \{0\} & c_1 \end{pmatrix}\begin{Bmatrix} \{\dot{d}_b\} \\ \{\dot{d}_a\} \\ \dot{y} \end{Bmatrix} + \begin{pmatrix} \mathscr{K}_{bb}(t) & \{0\} & \mathscr{K}_{by}(t) \\ \{0\} & \mathscr{K}_{aa} & \{0\} \\ \mathscr{K}_{yb}(t) & \{0\} & k_1 \end{pmatrix}\begin{Bmatrix} \{d_b\} \\ \{d_a\} \\ y \end{Bmatrix} + \begin{Bmatrix} [k_N] \\ \{0\} \end{Bmatrix}\begin{Bmatrix} \{d_b\} \\ \{d_a\} \\ y \end{Bmatrix} = \begin{Bmatrix} f_b(t) \\ \{0\} \\ 0 \end{Bmatrix}. \tag{6}$$

Upon the exit of the oscillator from the beam, that is, for $t \geqslant t_f$, the governing equation of motion reads

$$\begin{pmatrix} M & 0 \\ 0 & M_{aa} \end{pmatrix}\begin{Bmatrix} \{\ddot{d}_b\} \\ \{\ddot{d}_a\} \end{Bmatrix} + \begin{pmatrix} C & 0 \\ 0 & C_{aa} \end{pmatrix}\begin{Bmatrix} \{\dot{d}_b\} \\ \{\dot{d}_a\} \end{Bmatrix} + \begin{pmatrix} K & 0 \\ 0 & K_{aa} \end{pmatrix}\begin{Bmatrix} \{d_b\} \\ \{d_a\} \end{Bmatrix} + [k_N]\begin{Bmatrix} \{d_b\} \\ \{d_a\} \end{Bmatrix} = \begin{Bmatrix} 0 \\ 0 \end{Bmatrix}. \tag{7}$$

The initial conditions for these equations, at $t = t_f$, are obtained from solution of Eq. (6) at $t = t_f$. Appendix A provides the details of expressions for the elements of the structural matrices appearing in the above equations. It must be noted that the governing equations of motion, as given in Eqs. (6) and (7), constitute a set of coupled nonlinear ordinary differential equations (ODE) with time varying coefficients.

3. Problem of spatial incompleteness of measurements

The FE model developed in the previous section serves as the baseline model in the damage detection strategy considered in this paper. An important question that needs to be addressed in this context is the problem of spatial incompleteness of measured data. It can generally be expected that not all structure dofs, that are included in the FE model, can actually be measured. This is because of one or more of the following reasons:

- It is not easy to measure rotational dofs,
- Number of dofs that could be measured simultaneously is limited by the number of channels available in the measurement set-up, and
- Not all dofs need be accessible for measurement.

As a result, there exists a mismatch of dofs in analytical baseline model and the experimental model, which, in turn, poses significant difficulties in developing damage detection strategies. To deal with this difficulty, one could use a suitable FE model reduction scheme so that the dofs that are not measured are reduced in terms of the dofs that are measured. In this context it is of interest to note that the problem of nonlinear model reduction is widely encountered in the study of large scale nonlinear dynamical systems: see, for example, the works of Sirovich [27–29], Berkooz et al. [30], and Newman [31,32]. The review paper by Noor [33] on reduction methods addresses both mathematical aspects and applications to various areas including problems of nonlinear vibrations. The recent paper by Matthies and Meyer [34] contain extensive references to related literature. In the context of linear time-invariant FE model reduction, there exists several reduction schemes in the literature, such as, the static and dynamic condensation techniques [26] and system equivalent reduction and expansion process (SEREP) [35]. All these schemes, even when applied to linear time invariant systems, are essentially approximate in nature and are applied with the objective that the reduced model captures, to reasonable level of approximation, the main features of the original larger model. In the context of the problem on hand, as has been already noted, the model to be reduced is not only time varying but also nonlinear. Thus, when model reduction schemes such as SEREP are used here, they introduce further approximations. To proceed further, however, one needs to accept these additional approximations.

To implement the reduction schemes for the problem on hand, we assume that oscillator response $y(t)$ is measured and we designate all the beam dofs that are measured as master dofs and denote them by $d_m(t)$, and, the remaining beam dofs are called the slave dofs, and are denoted by $d_s(t)$. Thus, the beam dofs are partitioned as

$$\{d(t)\}^T = [\{d_m(t)\}\{d_s(t)\}]. \tag{8}$$

Accordingly, the beam mass, stiffness and modal matrices also get partitioned as

$$K = \begin{bmatrix} K_{mm} & K_{ms} \\ K_{sm} & K_{ss} \end{bmatrix},$$
$$M = \begin{bmatrix} M_{mm} & M_{ms} \\ M_{sm} & M_{ss} \end{bmatrix}, \tag{9}$$
$$[\Phi] = \begin{bmatrix} \Phi_m \\ \Phi_s \end{bmatrix}.$$

The reduction scheme here is proposed to be applied only to the beam dofs. The essence of all the alternative reduction schemes is to introduce the transformation

$$\{d(t)\} = [W]\{d_m(t)\}. \tag{10}$$

Here $[W]$ is the $n \times n_m$ transformation matrix that relates the $n \times 1$ beam dofs with the $n_m \times 1$ master dofs. For SEREP reduction, the transformation matrix reads

$$[W] = \begin{bmatrix} \Phi_m \\ \Phi_s \end{bmatrix} [\Phi_m^T \Phi_m]^{-1} \Phi_m^T. \tag{11}$$

In arriving at this transformation matrix, the displacement vector $\{d(t)\}$ is expressed in terms of the generalized coordinates $\{z(t)\}$ as $\{d(t)\} = [\Phi]\{z(t)\}$. Upon partitioning the displacement vector into master and slave dofs, as in Eq. (8), and partitioning the modal matrix as in Eq. (9), it follows that $\{d_m(t)\} = [\Phi_m]\{z(t)\}$ and $\{d_s(t)\} = [\Phi_s]\{z(t)\}$. This leads to the expression for the generalized coordinate vector $\{z(t)\} = [\Phi_m]^+\{d_m\}$ where $[\Phi_m]^+ = [\Phi_m^T \Phi_m]^{-1}[\Phi_m]^T$ is the pseudo-inverse of $[\Phi_m]$. This leads to the transformation matrix as given in Eq. (11). The relative merits of the above mentioned reduction schemes are widely discussed in the literature, see, for instance, the paper by Callahan et al. [35]. The accuracy of static and dynamic condensation techniques is affected by the choice of active dofs. On the other hand SEREP provides features, that the other two reduction schemes do not, such as [35]

- the arbitrary selection of modes that are to be preserved in the reduced system model,
- the quality of the reduced model is not dependent upon the location of the selected active dof, and
- the frequencies and the mode shapes of the reduced system are exactly equal to the frequencies and mode shapes (for the selected modes) of the full system model.

Upon reducing the dofs, as indicated in Eq. (10), the reduced mass, stiffness and damping matrices for the beam structure are obtained as

$$[M_r] = [W]^{\mathrm{T}}[M][W], \quad [K_r] = [W]^{\mathrm{T}}[K][W],$$
$$[C_r] = [W]^{\mathrm{T}}[C][W]. \tag{12}$$

Now, Eq. (6) can be written as

$$[\overline{M}_N]\begin{pmatrix}\{\ddot{d}\}\\ \{\ddot{d}_a\}\\ \ddot{y}\end{pmatrix} + [\overline{C}_N]\begin{pmatrix}\{\dot{d}_b\}\\ \{\dot{d}_a\}\\ \dot{y}\end{pmatrix} + [\overline{K}_N]\begin{pmatrix}\{d_b\}\\ \{d_a\}\\ y\end{pmatrix} + \begin{pmatrix}[k_N]\\ 0\end{pmatrix}\begin{pmatrix}\{d_b\}\\ \{d_a\}\end{pmatrix} = \{F\}. \tag{13}$$

See Appendix A for expressions for elements of above structural matrices. Upon applying the model reduction transformation, and premultiplying both side of equation $[W]^{\mathrm{T}}$, one gets

$$\begin{aligned}&[\overline{M}_{N_r}]\{\ddot{d}_{\mathrm{m}}\} + [\overline{C}_{N_r}]\{\dot{d}_{\mathrm{m}}\} + [\overline{K}_{N_r}]\{d_{\mathrm{m}}\}\\ &+ [W]^{\mathrm{T}}\begin{pmatrix}-k_1\left[N\left(x = v_0 t + \frac{1}{2}a_0 t^2\right)\right]^{\mathrm{T}}\\ \{0\}\end{pmatrix} y\\ &+ [W]^{\mathrm{T}}\begin{pmatrix}-c_1\left[N\left(x = v_0 t + \frac{1}{2}a_0 t^2\right)\right]^{\mathrm{T}}\\ \{0\}\end{pmatrix}\dot{y}\\ &+ \left([\bar{k}N_r]\{d_{\mathrm{m}}\}\right)\\ &= [W]^{\mathrm{T}}\begin{pmatrix}\left[N\left(x = v_0 t + \frac{1}{2}a_0 t^2\right)\right]^{\mathrm{T}}(m_1 + m_2)g\\ \{0\}\end{pmatrix},\end{aligned} \tag{14}$$

where

$$\begin{aligned}[\overline{M}_{N_r}] &= [W]^{\mathrm{T}}\begin{pmatrix}[M] + [m]^* & \{0\}\\ \{0\} & [M_{aa}]\end{pmatrix}[W],\\ [\overline{C}_{N_r}] &= [W]^{\mathrm{T}}\begin{pmatrix}[C] + [c]^* & \{0\}\\ \{0\} & [C_{aa}]\end{pmatrix}[W],\\ [\overline{K}_{N_r}] &= [W]^{\mathrm{T}}\begin{pmatrix}[K] + [k]^* & \{0\}\\ \{0\} & [K_{aa}]\end{pmatrix}[W],\\ [\bar{k}N_r] &= [W]^{\mathrm{T}}\{k_N\}[W],\end{aligned} \tag{15}$$

are the reduced structural matrices. Upon the exit of the oscillator, that is, for $t \geqslant t_{\mathrm{f}}$, after applying model reduction transformation, the governing equation of motion for beam–oscillator system reads

$$\begin{aligned}&[M_{N_a}][W]\{\ddot{d}_{\mathrm{m}}\} + [C_{N_a}][W]\{\dot{d}_{\mathrm{m}}\} + [K_{N_a}][W]\{d_{\mathrm{m}}\}\\ &+ \{k_N\}[W]\{d_{\mathrm{m}}\}\\ &= \{0\},\end{aligned} \tag{16}$$

where

$$\begin{aligned}[M_{N_a}] &= \begin{pmatrix}[M] & \{0\}\\ \{0\} & \sum_{k=1}^{n_{\mathrm{e}}} m_k \int_0^{l_k}[S(x)]_k^{\mathrm{T}}[S(x)]_k\,\mathrm{d}x\end{pmatrix},\\ [C_{N_a}] &= \begin{pmatrix}[C] & \{0\}\\ \{0\} & \sum_{k=1}^{n_{\mathrm{e}}} c_a \int_0^{l_k}[S(x)]_k^{\mathrm{T}}[S(x)]_k\,\mathrm{d}x\end{pmatrix},\\ [K_{N_a}] &= \begin{pmatrix}[K] & \{0\}\\ \{0\} & \sum_{k=1}^{n_{\mathrm{e}}} \mathrm{AE}_k \int_0^{l_k}\frac{\partial[S(x)]_k^{\mathrm{T}}}{\partial x}\frac{\partial[S(x)]_k}{\partial x}\,\mathrm{d}x\end{pmatrix}.\end{aligned}$$

Premultiplying both sides of Eq. (16) by $[W]^{\mathrm{T}}$, one gets

$$[M_{N_{ar}}]\{\ddot{d}_{\mathrm{m}}\} + [C_{N_{ar}}]\{\dot{d}_{\mathrm{m}}\}[K_{N_{ar}}]\{d_{\mathrm{m}}\}\{\bar{k}N_r\}\{d_{\mathrm{m}}\} = \{0\}, \tag{17}$$

where

$$\begin{aligned}[M_{N_{ar}}] &= [W]^{\mathrm{T}}[M_{N_a}][W],\\ [C_{N_{ar}}] &= [W]^{\mathrm{T}}[C_{N_a}][W],\\ [K_{N_{ar}}] &= [W]^{\mathrm{T}}[K_{N_a}][W],\\ \{\bar{k}N_r\} &= [W]^{\mathrm{T}}\{k_N\}[W].\end{aligned} \tag{18}$$

The reduced set of equations, as given in Eqs. (14) and (18), thus, again constitute a set of nonlinear ODEs with time varying coefficients.

4. Damage detection algorithm

Attention is focussed in the present study on two types of damage scenarios: Firstly, we assume that the flexural rigidity, EI_k, of the kth finite element of the beam, upon the occurrence of damage, becomes $\alpha_k \mathrm{EI}_k$. Secondly, we consider the possibility of the bearings becoming partially immobile. This is modeled by emergence of rotary stiffnesses, represented by the springs with stiffness $k_{\theta 1}$ and $k_{\theta 2}$, (see, Fig. 1) at the beam ends which otherwise are absent in an undamaged beam. The problem of damage detection, thus, can be stated as finding $(\alpha_k)_{k=1}^{n_{\mathrm{e}}}$, $k_{\theta 1}$ and $k_{\theta 2}$ based on measurement of $y(t_j)$, $\dot{y}(t_j)$, $\ddot{y}(t_j)$, $\{d(t_j)\}$, $\{\dot{d}(t_j)\}$, and $\{\ddot{d}(t_j)\}$ for $j = 1, 2, \ldots, s$. Here n_{e} = number of finite elements into which the beam structure is divided. Clearly, for the undamaged structure, $\alpha_k = 1$ for $k = 1, 2, \ldots, n_{\mathrm{e}}$ and $k_{\theta 1}$, $k_{\theta 2} = 0$. Thus, any departure in the values of α_k, from the reference value of unity, and, in the values of $k_{\theta 1}$ and $k_{\theta 2}$, from the reference value of zero, indicates the occurrence of damage. It is also clear that the determination of these variables also helps to locate the damage and also to quantify its severity. It is assumed in the present study that the characteristics of the oscillator, namely, m_1, m_2, c_1, k_1 and its velocity and acceleration are known. It is also assumed that the beam mass and damping matrices are unaffected by the occurrence of the damage and hence are taken to be known a priori.

To describe the damage detection algorithm, we begin by considering the case of $k_{\theta 1} = k_{\theta 2} = 0$. The beam itself is taken to have undergone changes in its flexural rigidity. The stiffness matrix of the damaged beam structure is expressed in the form

$$K = \sum_{k=1}^{n_{\mathrm{e}}} \alpha_k [A]_k^{\mathrm{T}}[\overline{K}]_k[A]_k. \tag{19}$$

Here $[\overline{K}]_i$ = the ndof × ndof stiffness matrix of the ith element in its undamaged state in the global coordinate

system and $[A]_k$ = the ndof$\times n$ matrix of extended element nodal displacement that facilitates automatic assembling of global stiffness matrix from the constituent element stiffness matrix. Based on the values of the beam and oscillator responses measured at $t = t_j$, Eq. (14) can be recast to read

$$\begin{aligned}&(\,[\overline{K}_{N_r}] + [\bar{k}N_r]\,)\{d_{\mathrm{m}}(t_j)\}\\ &\quad = [W]^{\mathrm{T}}\begin{pmatrix}[N(x)]^{\mathrm{T}}(m_1+m_2)g\\ \{0\}\end{pmatrix} - [\overline{M}_{N_r}]\times\{\ddot{d}_{\mathrm{m}}(t_j)\}\\ &\qquad - [\overline{C}_{N_r}]\{\dot{d}_{\mathrm{m}}(t_j)\}\\ &\qquad - [W]^{\mathrm{T}}\begin{pmatrix}-k_1\left[N\left(x=v_0t+\frac{1}{2}a_0t^2\right)\right]^{\mathrm{T}}\\ \{0\}\end{pmatrix}y(t_j)\\ &\qquad - [W]^{\mathrm{T}}\begin{pmatrix}-c_1\left[N\left(x=v_0t+\frac{1}{2}a_0t^2\right)\right]^{\mathrm{T}}\\ \{0\}\end{pmatrix}\dot{y}(t_j),\quad 0\leqslant t\leqslant t_{\mathrm{f}}\end{aligned} \tag{20}$$

and

$$[K_{N_{ar}}] + \{\bar{k}N_r\}\{d_{\mathrm{m}}\} = -[M_{N_{ar}}]\{\ddot{d}_{\mathrm{m}}\} - [C_{N_{ar}}]\{\dot{d}_{\mathrm{m}}\},\quad t\geqslant t_{\mathrm{f}}. \tag{21}$$

This can be simplified to read

$$(\,[\overline{K}_{N_r}] + [\bar{k}N_r]\,)(\,\{d_{\mathrm{m}}(t_j)\}\,) = F_r(t_j),\quad 0\leqslant t\leqslant t_{\mathrm{f}} \tag{22}$$

and

$$(\,[\overline{K}_{N_{ar}}] + [\bar{k}N_r]\,)(\,\{d_{\mathrm{m}}(t_j)\}\,) = F_r(t_j),\quad t\geqslant t_{\mathrm{f}}, \tag{23}$$

where

$$\begin{aligned}F_r(t_j) &= [W]^{\mathrm{T}}\begin{pmatrix}\left[N\left(x=v_0t_j+\frac{1}{2}a_0t_j^2\right)\right]^{\mathrm{T}}(m_1+m_2)g\\ \{0\}\end{pmatrix}\\ &\quad - [\overline{M}_{N_r}]\{\ddot{d}_{\mathrm{m}}(t_j)\} - [\overline{C}_{N_r}]\{\dot{d}_{\mathrm{m}}(t_j)\}\\ &\quad - [W]^{\mathrm{T}}\begin{pmatrix}-k_1\left[N\left(x=v_0t_j+\frac{1}{2}a_0t_j^2\right)\right]^{\mathrm{T}}\\ \{0\}\end{pmatrix}y(t_j)\\ &\quad - [W]^{\mathrm{T}}\begin{pmatrix}-c_1\left[N\left(x=v_0t_j+\frac{1}{2}a_0t_j^2\right)\right]^{\mathrm{T}}\\ \{0\}\end{pmatrix}\dot{y}(t_j),\\ &\quad 0\leqslant t\leqslant t_{\mathrm{f}},\end{aligned} \tag{24}$$

$$F_r(t_j) = -[M_{N_{ar}}]\{\ddot{d}_{\mathrm{m}}(t_j)\} - [C_{N_{ar}}]\{\dot{d}_{\mathrm{m}}(t_j)\},\quad t\geqslant t_{\mathrm{f}}. \tag{25}$$

Using Eq. (19), Eq. (22) can be recast as

$$\mathscr{B}_{\mathrm{m}}(t_j)\}\sum_{k=1}^{n_{\mathrm{e}}}\alpha_k = \{F_r(t_j)\}, \tag{26}$$

where $\{B_{\mathrm{m}}(t_j)\}$ is a $n_{\mathrm{m}}\times n_{\mathrm{e}}$ matrix given by

$$\{\mathscr{B}_{\mathrm{m}}(t_j)\} = [W]^{\mathrm{T}}\left\{\sum_{k=1}^{n_{\mathrm{e}}}[A]_k^{\mathrm{T}}([\overline{K}_{N_r}] + [\bar{k}N_r])_k[A]_k\right\}[W]\{d_{\mathrm{m}}(t_j)\},\quad 0\leqslant t\leqslant t_{\mathrm{f}} \tag{27}$$

and

$$\{\mathscr{B}_{\mathrm{m}}(t_j)\} = [W]^{\mathrm{T}}\left\{\sum_{k=1}^{n_{\mathrm{e}}}[A]_k^{\mathrm{T}}([\overline{K}_{N_{ar}}] + [\bar{k}N_r])_k[A]_k\right\}[W]\{d_{\mathrm{m}}(t_j)\},\quad t\geqslant t_{\mathrm{f}}. \tag{28}$$

Eq. (26) can also be written as

$$\mathscr{B}_{\mathrm{m}}(t_j)\{\alpha\} = \{F_r(t_j)\}. \tag{29}$$

Here $\{\alpha\}$ is the $n_{\mathrm{e}}\times 1$ vector of damage indicator factors. If the response measurements are made for the time instants $t = t_1, t_2, \ldots, t_{\mathrm{s}}$, equations governing α, as given by Eq. (29), can be written for each of these time instants. Consequently, one gets the reduced set of equations:

$$[\mathscr{L}_{\mathrm{m}}]\{\alpha\} = \{\mathscr{F}_r\}, \tag{30}$$

where $[\mathscr{L}_{\mathrm{m}}]$ is a $sn_{\mathrm{m}}\times n_{\mathrm{e}}$ matrix given by

$$[\mathscr{L}_{\mathrm{m}}]^{\mathrm{T}} = [\mathscr{B}_{\mathrm{m}}(t_1)\mathscr{B}_{\mathrm{m}}(t_2)\cdots\mathscr{B}_{\mathrm{m}}(t_{\mathrm{s}})] \tag{31}$$

and $\{\mathscr{F}_{\mathrm{m}}\}$ is a $sn_{\mathrm{m}}\times 1$ vector given by

$$\{\mathscr{F}_{\mathrm{m}}\}^{\mathrm{T}} = [F_r(t_1)F_r(t_2)\cdots F_r(t_{\mathrm{s}})]. \tag{32}$$

Eq. (30) represents sn_{m} number of equations for the unknowns α_k, $k = 1, 2, \ldots, n_{\mathrm{e}}$. Since the transformation matrix W is a nonlinear function of α, it follows that Eq. (30) constitutes a set of overdetermined nonlinear algebraic equations. To obtain an approximation to α we follow an iterative strategy. This involves the following steps:

Step 1. Determine the first approximation to W from the structural matrices of the undamaged structure. Obtain an initial approximation $\tilde{\alpha}$ to α using the equation

$$\{\alpha\} = [\mathscr{L}_{\mathrm{m}}]^{+}\{\mathscr{F}_r\}, \tag{33}$$

where $[\mathscr{L}_{\mathrm{m}}]^{+}$ is the left pseudo-inverse given by

$$[\mathscr{L}_{\mathrm{m}}]^{+} = [\mathscr{L}_{\mathrm{m}}^{\mathrm{T}}\mathscr{L}_{\mathrm{m}}]^{-1}\mathscr{L}_{\mathrm{m}}^{\mathrm{T}}. \tag{34}$$

Step 2. Determine the modified structure stiffness matrix by treating $\tilde{\alpha}$ as an approximation to α. Determine the modal matrix $[\Phi]$ and hence the updated transformation matrix W using Eq. (11).

Step 3. Update the estimate of α using the improved estimate of W obtained in step 2.

Repeat steps 1–3 till satisfactory convergence on α is obtained. In the numerical work it was generally observed that acceptable convergence (with a tolerance of

10^{-04} on elements of α) was reached within about 3–5 iterations.

The above equations for the damage indicator factors α have been derived by assuming that $k_{\theta 1}, k_{\theta 2} = 0$. This would mean that the above procedure would not apply to detect the possibility of the bearings becoming partially immobile. In this context it must be noted that the damage indicator factor, α_k, essentially multiplies the stiffness parameter in the undamaged state to yield the corresponding stiffness parameter in the damaged state. Since, in the undamaged state $k_{\theta 1} = 0$ and $k_{\theta 2} = 0$, introducing a multiplying parameter to detect a nonzero $k_{\theta 1}$ and $k_{\theta 2}$ is clearly infeasible. To overcome this difficulty, the notion of a reference structure is introduced. This structure has two hypothetical rotary springs, with respective stiffnesses $k^*_{\theta 1}$ and $k^*_{\theta 2}$, attached to it at the two ends. To detect the possibility of bearings becoming partially immobile, two parameters α_{l} and α_{r} are introduced, such that, the bearing stiffness against rotation in the damaged state is given by

$$k_{\theta 1} = \alpha_{\mathrm{l}} k^*_{\theta 1}, \quad k_{\theta 2} = \alpha_{\mathrm{r}} k^*_{\theta 2}. \tag{35}$$

With this additional feature, the detection of damage can now be carried out using the steps as described in deriving Eq. (33). The damage indicator vector α in this case reads

$$\alpha = \{\alpha_1 = \alpha_{\mathrm{l}}, \alpha_2, \ldots, \alpha_{n-1}, \alpha_n = \alpha_{\mathrm{r}}\}. \tag{36}$$

Clearly, the estimates of α_{l} and α_{r} depend upon the values chosen for the reference parameters $k^*_{\theta 1}$ and $k^*_{\theta 2}$. To make an optimal choice, a nondimensional quantity,

$$\epsilon(k^*_{\theta 1}, k^*_{\theta 2}) = \sum_{j=1}^{n} \sum_{i=1}^{s} \frac{\{d_j(t_i, k^*_{\theta 1}, k^*_{\theta 2}) - d^M_j(t_i)\}^2}{[d^M_j(t_i)]^2} \tag{37}$$

is introduced. Here $d_j(t_i, k^*_{\theta 1}, k^*_{\theta 2})$ = estimated displacement at jth dof at $t = t_i$ with $k_{\theta 1} = k^*_{\theta 1}$, $k_{\theta 2} = k^*_{\theta 2}$ and $d^M_j(t_i)$ = measured response of the damaged structure at jth dof at time $t = t_i$. The best choice for $k^*_{\theta 1}$ and $k^*_{\theta 2}$ is taken to be the one that minimizes $\epsilon(k^*_{\theta 1}, k^*_{\theta 2})$. This minimization itself could be carried out by conducting a parametric study on $\epsilon(k^*_{\theta 1}, k^*_{\theta 2})$ by varying $k_{\theta 1}$ and $k_{\theta 2}$.

5. Numerical results and discussion

The formulation presented above is illustrated with reference to the beam–oscillator system shown in Fig. 1. It is assumed that the beam has uniform cross sectional properties with $L = 45$ m, $\mathrm{EI} = 1.62 \times 10^{11}$ N m^2, $\mathrm{AE} = 3.88 \times 10^{11}$ N, $m = 4625$ kg/m, $c = 1850$ N s/m, $c_a = 1$ N s/m. For the oscillator, it is assumed that $m_1 = m_2 = 500$ kg, $k_1 = 40 \times 10^7$ N/m and $c_1 = 160$ N s/m. The oscillator is assumed to travel with a velocity of 15 m/s and acceleration $a = 0$. The synthetic data that double for actual measurements are generated by integrating Eq. (6) using a fourth order Runge–Kutta procedure that is embedded into the ODE45 subroutine of the MATLAB software. In this calculation, the relative tolerance and the vector of absolute error tolerance, that the ODE45 subroutine requires as inputs, have been set at 10^{-3} and 10^{-6}, respectively. This ODE solver reports the response at time steps at which the specified tolerances are met. In implementing the proposed damage detection algorithm it is required to choose time windows over which the vibration data is gathered and, also, the time step at which the data is discretized. In the numerical work it was found that data window over $0 < t \leqslant 1.5t_{\mathrm{f}}$, where t_{f} = time that the vehicle spends on the bridge, lead to satisfactory performance of the damage detection algorithm. The data beyond $t \geqslant 1.5t_{\mathrm{f}}$, represents free vibration decay of the beam to increasingly lower values, and, hence, were found to provide no useful information on the influence of beam damage on the response. Furthermore, in discretizing the time for the purpose of damage detection, the time steps at which the ODE solver reported the response were themselves used. Typically, it was observed that, for a set of 12 damage indicator factors, the number of equations that lead to satisfactory convergence were of the order of 8000–12,000. Similarly, in calculation of $\epsilon(k^*_{\theta 1}, k^*_{\theta 2})$, as given by Eq. (37), the summation on t_i was taken over all the time instants at which the response time histories were discretized.

As can be seen from Fig. 2, there are five beam elements used in the spatial discretization and, consequently, the size of vector α in this case would be 12×1 with α_1 corresponding to the rotary spring k_{θ_1}, α_2–α_6, respectively corresponding to flexural rigidities $\{\mathrm{EI}_k\}_{k=1}^{5}$, α_7 corresponding to rotary spring k_{θ_2}, and α_7–α_{12}, respectively corresponding to axial rigidities. Thus, introducing the vector

$$\lambda^{\mathrm{T}} = \{k_{\theta 1}, \mathrm{EI}_1, \mathrm{EI}_2, \mathrm{EI}_3, \mathrm{EI}_4, \mathrm{EI}_5, k_{\theta 2}, \mathrm{AE}_1, \mathrm{AE}_2, \mathrm{AE}_3, \mathrm{AE}_4, \mathrm{AE}_5\},$$

we get

$$\{\lambda\}_{\mathrm{damaged}} = I\alpha\{\lambda\}_{\mathrm{undamaged}}, \tag{38}$$

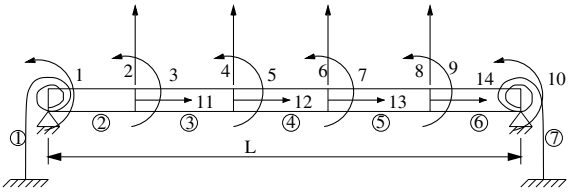

Fig. 2. Nonlinear FE model of the damaged beam that includes axial dofs. Numbers within the circles indicate the element number.

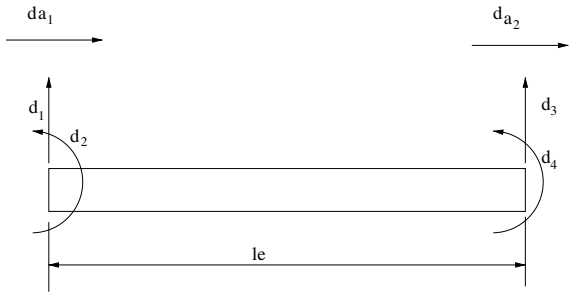

Fig. 3. kth beam element showing displacements at the nodal coordinates; the element has flexural rigidity $\mathrm{EI}(x)$, axial rigidity $\mathrm{AE}(x)$, and mass/unit length $m(x)$.

where, I is an identity matrix of size equal to number of rows in λ. As a prelude to the illustration of damage detection procedures, in Figs. 4 and 5, we examine the performance of model reduction schemes (Section 3) as applied to problem on hand. The results in these figures correspond to the case of master dofs being 2, 4, 11, and 12. The results from SEREP and Guyan's reduction for one of the master dof (midspan transverse deflection) and one of the slave dof (midspan rotation) are shown, respectively, in Figs. 4 and 5. In obtaining results from SEREP scheme, the first four modes are included in the reduction. As can be seen from these figures, the SEREP scheme performs relatively better than other schemes.

The different aspects of the damage detection procedure are illustrated with the help of the following case studies.

5.1. Studies on undamaged beam

We begin by considering the case in which vibration data emerges from an undamaged beam–oscillator system. The objective here are as follows:

- To ascertain that the damage detection algorithm does not report false alarms when vibration data is from an undamaged structure,
- To quantify the effect of model reduction on the ability of the damage detection algorithm to report no false alarms, and
- To demonstrate the importance of including geometric nonlinearity in the implementation of damage detection.

Thus, for the case, when the proposed algorithm was used in conjunction with vibration data from undamaged structure, the damage indicator vector α was obtained to be

$$\alpha^{\mathrm{T}} = \{1.0000, 0.9924, 0.9959, 0.9954, 0.9912, 0.9992, 1.0000, 1.0032, 1.0101, 0.9983, 0.9995, 1.0002\}.$$

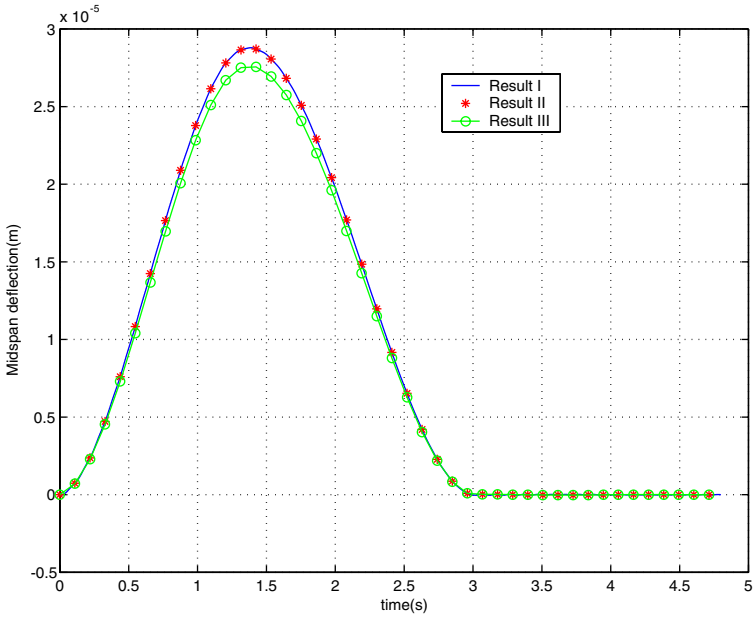

Fig. 4. Comparison between measured response from full non-linear analytical model and estimated response from reduced model using different reduction techniques, for master dof 4 (deflection at mid span) of beam–oscillator structure; Result I: measured response from full non-linear analytical model; Result II: estimated response from reduced model using SEREP; Result III: estimated response from reduced model using Guyan's reduction technique.

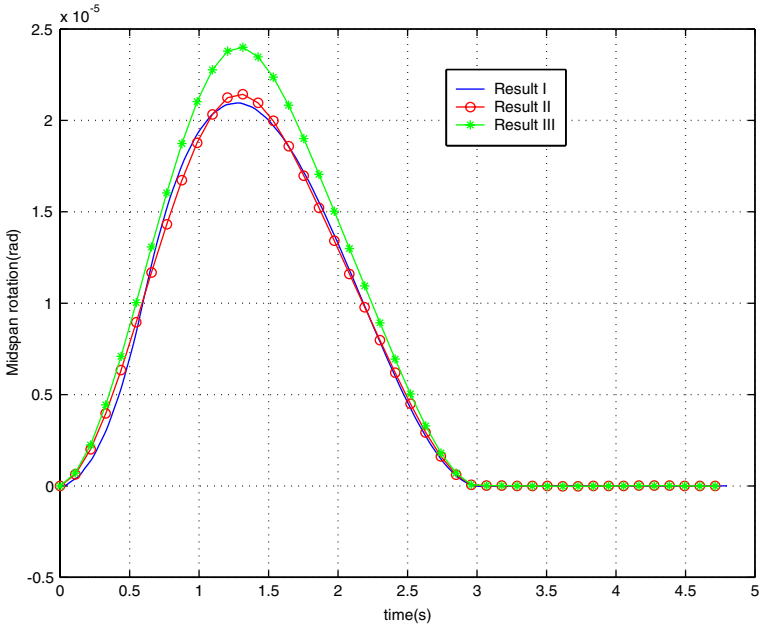

Fig. 5. Comparison between measured response from full non-linear analytical model and estimated response from reduced model, using different reduction techniques, for slave dof 5 (roatation at mid span) of beam–oscillator structure; Result I: measured response from full non-linear analytical model; Result II: estimated response from reduced model using SEREP; Result III: estimated response from reduced model using Guyan's reduction technique.

In this calculation, the reference values $k^*_{\theta_1}$ and $k^*_{\theta_2}$ were both obtained to be equal to 1.83×10^{-8} N m/rad. It follows that the maximum error of damage detection $\varepsilon_{\max} = 0.76\%$. Next, we consider damage detection in which the dofs 2, 4, 11, 12 (Fig. 2) are treated as master dofs and the rest as slave dofs and the SEREP reduction scheme with first four modes is employed. The damage indicator factor in this case turns out to be

$$\alpha^{\mathrm{T}} = \{1.0000, 0.9919, 0.9950, 0.9918, 0.9912, 0.9989, 1.0000, 1.0032, 1.0121, 0.9903, 0.9995, 1.0011\}$$

with $k^*_{\theta 1} = k^*_{\theta 2} = 1.83 \times 10^{-8}$ N m/rad. It can be observed that $\varepsilon_{\max} = 1.21\%$. Thus, the effect of model reduction is seen to result in an increase in $\varepsilon_{\max}$ from 0.76 to 1.21% which we believe is acceptable. This indicates that, to an acceptable level of accuracy, the structure is undamaged, as indeed is the case.

To study the difference that the presence of structural geometric nonlinearity makes in structural damage detection, results from a nonlinear undamaged structure (see, Fig. 6) are input to damage detection algorithm that ignores geometric nonlinearity effects. This algorithm forms a specific case of the formulation presented in Section 4 and this has been discussed in greater detail in Ref. [22]. Since, in a linear finite element model for beam–oscillator system, there exists no coupling between bending and axial deformation of the beam, the associated damage detection algorithm also does not provide indicators on values of axial stiffnesses. The linear algorithm predicts that the beam parameters are $\{EI_1, EI_2, EI_3, EI_4, EI_5\} = \{1.668\times10^{11}, 1.684\times10^{11}, 1.817\times10^{11}, 2.151\times10^{11}, 1.801\times10^{11}\}$ N m^2. Thus, in this case, it turns out that $\varepsilon_{\max} = 32.7\%$ which clearly demonstrates that the linear damage detection algorithm shows a significant false alarm and, hence, is inapplicable to the present problem.

5.2. Studies on damaged beam

To demonstrate the efficacy of proposed damage detection algorithm, we consider three scenarios of occurrence of damage:

Damage scenario 1

Here we assume that two bearings become partially immobile leading to $k_{\theta_1} = k_{\theta_2} = 4.00 \times 10^{11}$ N m/rad. The master dofs are taken to be 2, 4, 11, 12, and first four modes are employed in SEREP reduction. The damage indicator vector in this case is obtained as

$$\alpha^{\mathrm{T}} = \{0.9900, 0.9903, 0.9953, 0.9907, 0.9950, 1.0019, 1.0002, 0.9980, 0.9966, 0.9959, 0.9997, 0.9998\}$$

with $\varepsilon_{\max} = 1.0\%$ and $k^*_{\theta 1} = k^*_{\theta 2} = 4.00 \times 10^{11}$ N m/rad.

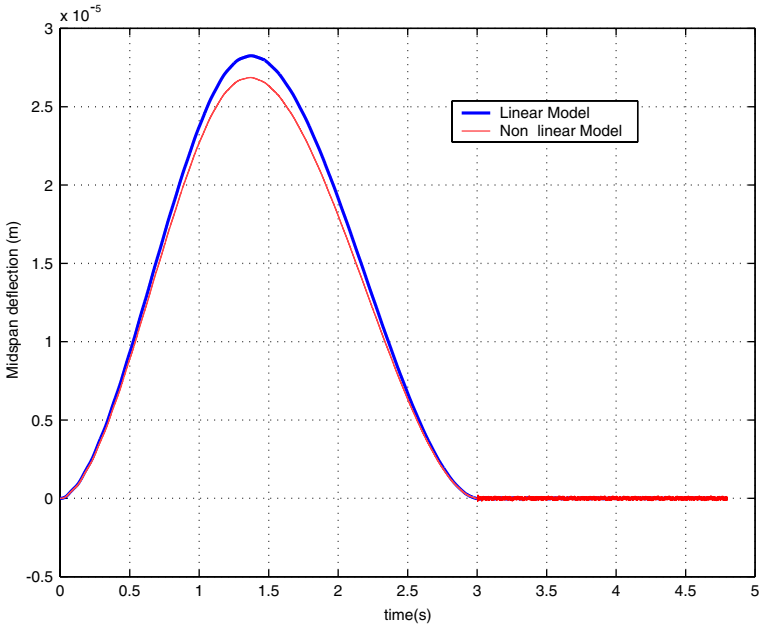

Fig. 6. Transverse deflection at midspan for undamaged structure obtained using full FE model: Result I, linear model; Result II, nonlinear model.

Damage scenario 2

Fig. 7 shows the damaged structure with one of the bearings becoming immobile and one of the beam elements developing 5% of loss of stiffness in both axial and flexural directions. The first four columns of Table 1 show actual beam parameters together with the corresponding estimates obtained using linear damage detection theory and nonlinear damage detection theory. As has been noted already, prediction of axial stiffness is

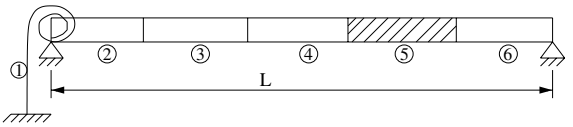

Fig. 7. Beam with immobile bearing restraints $k_{\theta_1} = 4.0 \times 10^{11}$ N m/rad; $k_{\theta_2} = 0.0$; the hatched portion refers to damaged beam element with 5% reduction in EI and AE in the fifth element.

Table 1
Results of damage detection for damage scenarios 2 and 3

Beam parameters	Damage scenario 2 (Fig. 7)			Damage scenario 3 (Fig. 8)		
	Actual values	Detected values from full linear model	Detected values from full nonlinear model	Actual values	Detected values from full nonlinear model	Detected values from reduced nonlinear model
k_{θ_1} (N m/rad)	4.0000×10^{11}	4.0003×10^{11}	4.0003×10^{11}	4.0000×10^{11}	3.961×10^{11}	4.0005×10^{11}
EI_1 (N m^2)	1.621×10^{11}	2.091×10^{11}	1.605×10^{11}	1.621×10^{11}	1.607×10^{11}	1.605×10^{11}
EI_2 (N m^2)	1.621×10^{11}	1.684×10^{11}	1.606×10^{11}	1.539×10^{11}	1.533×10^{11}	1.545×10^{11}
EI_3 (N m^2)	1.621×10^{11}	1.990×10^{11}	1.612×10^{11}	1.621×10^{11}	1.613×10^{11}	1.606×10^{11}
EI_4 (N m^2)	1.539×10^{11}	2.074×10^{11}	1.530×10^{11}	1.621×10^{11}	1.626×10^{11}	1.631×10^{11}
EI_5 (N m^2)	1.621×10^{11}	1.843×10^{11}	1.632×10^{11}	1.459×10^{11}	1.458×10^{11}	1.458×10^{11}
$k_{\theta 2}$ (N m/rad)	0.0	1.832×10^{-8}	1.822×10^{-8}	0.0	1.822×10^{-8}	1.822×10^{-8}
AE_1 (N)	3.881×10^{11}	–	3.884×10^{11}	3.881×10^{11}	3.871×10^{11}	3.892×10^{11}
AE_2 (N)	3.881×10^{11}	–	3.876×10^{11}	3.687×10^{11}	3.656×10^{11}	3.682×10^{11}
AE_3 (N)	3.881×10^{11}	–	3.873×10^{11}	3.881×10^{11}	3.855×10^{11}	3.8778×10^{11}
AE_4 (N)	3.686×10^{11}	–	3.681×10^{11}	3.881×10^{11}	3.893×10^{11}	3.871×10^{11}
AE_5 (N)	3.881×10^{11}	–	3.849×10^{11}	3.493×10^{11}	3.496×10^{11}	3.493×10^{11}

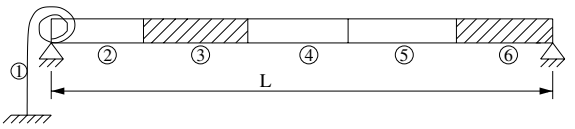

Fig. 8. Beam with immobile bearing restraints $k_{\theta_1} = 4.0 \times 10^{11}$ N m/rad; $k_{\theta_2} = 0.0$; the hatched portions refer to damaged beam elements with 5% reduction in EI and AE in the third element and 10% reduction in EI and AE in the sixth element.

not possible using linear damage detection algorithm, and, consequently, these values are not reported. In these calculations it was observed that $k^*_{\theta 1} = 4.00 \times 10^{11}$ N m/rad and $k^*_{\theta 2} = 1.83 \times 10^{-8}$ N m/rad. It was also observed that $\varepsilon_{\max} = 34.74\%$ for linear damage detection and 0.81% for nonlinear damage detection algorithm. This, again, clearly demonstrates the need to include geometric nonlinear effects in damage detection for the example structure studied herein.

Damage scenario 3

The damage scenario assumed here is as shown in Fig. 8. Here, one of the bearings is taken to be immobile and the beam is taken to suffer loss of axial and bearing stiffness at two different places. The values of the actual beam parameters, together with corresponding values predicted from damage detection algorithm using full and reduced nonlinear models, are shown in the columns 5–7 of Table 1. In the reduced model, as before, the dofs 2, 4, 11, 12 are taken as master dofs and first four modes are included in SEREP. The maximum error of damage detection using full FE model and the reduced FE model were observed to be approximately equal with $\varepsilon_{\max} = 0.97\%$. These errors however are observed to occur at two different locations (in element 4 for full finite element model and in element 2 for reduced FE model). This points towards the efficacy of SEREP scheme in model reduction. The reference values of rotary spring in these calculation were found to be $k^*_{\theta 1} = 4.00 \times 10^{11}$ N m/rad and $k^*_{\theta 2} = 1.83 \times 10^{-8}$ N m/rad.

6. Conclusions

A time domain approach, within the framework of FE modeling, has been developed in this study to detect damages in beam structures using data on vibration induced by a moving oscillator. In studies of this kind it is important to recognize that the accuracy of damage detection crucially depends upon the ability of FE model employed to capture changes in structural response caused due to damages. This calls for greater sophistication in FE modeling than what perhaps is needed in problems of response prediction. The study reported in this paper accounts for a few complicating features associated with response of beam–oscillator system. This includes the effects due to nonlinear dynamic interaction between oscillator and beam and spatial incompleteness of the measured data. Specifically, we have limited our attention to the nonlinear effects that emanate from nonlinear strain–displacement relations for the beam structure. The governing equations of motion in this case constitute a set of coupled nonlinear differential equations with time varying coefficients. Consequently, the damage detection problem is not amenable for solution using modal domain techniques. The time domain approach developed in this study leads to a set of overdetermined linear algebraic equations for the damage indicator variables which is solved using matrix pseudo-inverse theory. An interesting feature of this formulation is that the governing equation for damage indicator factor α remains linear as long as the measurements made are spatially complete. This is true, not withstanding the fact that the structure behaves nonlinearly. Of course, when measurements are spatially incomplete, as is going to be the case in most practical applications, the governing equation for α becomes nonlinear in nature and needs an iterative strategy for its solution. The limited set of numerical illustrations reported in this paper demonstrates the accuracy of the method developed. Using the procedures recommended in this study, the maximum error that is found to occur in detection of damage is seen to remain less than about 1.5% for all the cases reported in this investigation. To extend the scope of the present study to address real life problems, the following further studies need to be conducted:

- The development of the proposed damage detection algorithm when elaborate FE models for the bridge–vehicle structures are considered.
- Development of the algorithm to incorporate the effect of noise in the measurement of bridge–vehicle responses and other sources of uncertainties such as guideway unevenness, environmental effects such as presence of wind and temperature changes. This study can be carried out within the framework of theory of stationary random processes and perturbation formalisms. In the context of damage detection using linear vehicle structure interactions, the present authors have reported in Ref. [22] a first order perturbation method to predict random variabilities in damage indication factors due to measurement noise. The extension of this work to include nonlinear vehicle-structure interactions needs to be conducted.
- Inclusion of material nonlinearity, vehicle suspension nonlinearity and nonlinearities due to loss of contact between beam and oscillator in the damage detection algorithm.
- To validate the algorithm developed based on experimental/field studies.

Work on achieving these extensions is currently being conducted by the present authors.

Acknowledgement

The work reported in this paper has been supported by funding from the Council for Scientific & Industrial Research, Government of India.

Appendix A

Elements of mass matrix appearing in Eqs. (6) *and* (13):

$$M_{bb(t)} = \sum_{k=1}^{n_e} m_k \sum_{r=1}^{n_d} \int_0^{l_k} [N_r(\varsigma)]_k^T [N_r(\varsigma)]_k \, d\varsigma + \sum_{k=1}^{n_e} m_2 \sum_{r=1}^{n_d} \left[N_r\left(v_0 t + \frac{1}{2} a_0 t^2\right)\right]_k^T \times \left[N_r\left(v_0 t + \frac{1}{2} a_0 t^2\right)\right], \tag{A.1}$$

$$M_{aa} = \sum_{k=1}^{n_e} m_k \sum_{z=1}^{m_d} \int_0^{l_k} [S_z(\varsigma)]_k^T [S_z(\varsigma)]_k \, d\varsigma, \tag{A.2}$$

$$[m]^* = \sum_{k=1}^{n_e} m_2 \sum_{r=1}^{n_d} \left[N_r\left(v_0 t + \frac{1}{2} a_0 t^2\right)\right]_k^T \left[N_r\left(v_0 t + \frac{1}{2} a_0 t^2\right)\right]_k. \tag{A.3}$$

Elements of damping matrix appearing in Eqs. (6) *and* (13):

$$C_{bb(t)} = \sum_{k=1}^{n_e} c \sum_{r=1}^{n_d} \int_0^{l_k} [N_r(\varsigma)]_k^T [N_r(\varsigma)]_k \, d\varsigma + \sum_{k=1}^{n_e} c_1 \sum_{r=1}^{n_d} \left[N_r\left(v_0 t + \frac{1}{2} a_0 t^2\right)\right]_k^T \times \left[N_r\left(v_0 t + \frac{1}{2} a_0 t^2\right)\right]_k + 2m_2 \dot{\varsigma} \times \left[N_r\left(v_0 t + \frac{1}{2} a_0 t^2\right)\right]_{\varsigma_k} \left[N_r\left(v_0 t + \frac{1}{2} a_0 t^2\right)\right]_k^T, \tag{A.4}$$

$$C_{by(t)} = -\sum_{k=1}^{n_e} c_1 \sum_{r=1}^{n_d} \left[N_r\left(\varsigma = v_0 t + \frac{1}{2} a_0 t^2\right)\right]_k, \tag{A.5}$$

$$C_{aa} = \sum_{k=1}^{n_e} c_a \sum_{z=1}^{m_d} \int_0^{l_k} [S_z(\varsigma)]_k^T [S_z(\varsigma)]_k \, d\varsigma, \tag{A.6}$$

$$[c]^* = \sum_{k=1}^{n_e} c_1 \sum_{r=1}^{n_d} \left[N_r\left(v_0 t + \frac{1}{2} a_0 t^2\right)\right]_k^T \left[N_r\left(v_0 t + \frac{1}{2} a_0 t^2\right)\right]_k + \sum_{k=1}^{n_e} 2m_2 (v_0 + a_0 t) \sum_{r=1}^{n_d} \left[N_r\left(\varsigma = v_0 t + \frac{1}{2} a_0 t^2\right)\right]_{\varsigma_k} \times \left[N_r\left(v_0 t + \frac{1}{2} a_0 t^2\right)\right]_k^T. \tag{A.7}$$

Elements of stiffness matrix appearing in Eqs. (6) *and* (13):

$$K_{bb(t)} = \sum_{k=1}^{n_e} EI_k \sum_{r=1}^{n_d} \int_0^{l_k} \frac{\partial^2 [N_r(\varsigma)]_k^T}{\partial \varsigma^2} \frac{\partial^2 [N_r(\varsigma)]_k}{\partial \varsigma^2} \, d\varsigma + \sum_{k=1}^{n_e} k_1 \sum_{r=1}^{n_d} \left[N_r\left(\varsigma = v_0 t + \frac{1}{2} a_0 t^2\right)\right]_k^T \times \left[N_r\left(\varsigma = v_0 t + \frac{1}{2} a_0 t^2\right)\right]_k + \sum_{k=1}^{n_e} c_1 \sum_{r=1}^{n_d} \left[N_r\left(\varsigma = v_0 t + \frac{1}{2} a_0 t^2\right)\right]_k^T (v_0 + a_0 t) \times \left[N_r\left(\varsigma = v_0 t + \frac{1}{2} a_0 t^2\right)\right]_{\varsigma_k} + \sum_{k=1}^{n_e} m_2 t^2 \sum_{r=1}^{n_d} \left[N_r\left(\varsigma = v_0 t + \frac{1}{2} a_0 t^2\right)\right]_k^T \times \left[N_r\left(\varsigma = v_0 t + \frac{1}{2} a_0 t^2\right)\right]_{\varsigma\varsigma_k} + \sum_{k=1}^{n_e} m_2 a_0 \sum_{r=1}^{n_d} [N_r(\varsigma)]_k^T \left[N_r\left(\varsigma = v_0 t + \frac{1}{2} a_0 t^2\right)\right]_{\varsigma_k}, \tag{A.8}$$

$$K_{by(t)} = -\sum_{k=1}^{n_e} k_1 \sum_{r=1}^{n_d} \left[N_r\left(v_0 t + \frac{1}{2} a_0 t^2\right)\right]_k, \tag{A.9}$$

$$K_{aa} = \sum_{k=1}^{n_e} AE_k \sum_{z=1}^{m_d} \int_0^{l_k} \frac{\partial [S_z(\varsigma)]_k^T}{\partial \varsigma} \frac{\partial [S_z(\varsigma)]_k}{\partial \varsigma} \, d\varsigma, \tag{A.10}$$

$$K_{yb(t)} = -\sum_{k=1}^{n_e} c_1 \sum_{r=1}^{n_d} (v_0 + a_0 t) \left[N_r\left(\varsigma = v_0 t + \frac{1}{2} a_0 t^2\right)\right]_{\varsigma_k} - \sum_{k=1}^{n_e} k_1 \sum_{r=1}^{n_d} \left[N_r\left(v_0 t + \frac{1}{2} a_0 t^2\right)\right]_k, \tag{A.11}$$

$$[k_N] \begin{Bmatrix} \{d_b\} \\ \{d_a\} \end{Bmatrix} = \left\{ \sum_{k=1}^{n_e} \left\{ AE_k \sum_{r=1}^{n_d} \int_0^{l_k} \frac{\partial [N_r(\varsigma)]_k^T}{\partial \varsigma} \times \left[\frac{\partial [S_z(\varsigma)]_k}{\partial \varsigma} \{d_a r\}^k + \sum_{r=1}^{n_d} \frac{1}{2} \{d_r\}^{k^T} \times \frac{\partial [N_r(\varsigma)]_k^T}{\partial \varsigma} \frac{\partial [N_r(\varsigma)]_k}{\partial \varsigma} \{d_r\}^k \right] \frac{\partial [N_r(\varsigma)]_k}{\partial \varsigma} \right\} d\varsigma \{d_r\}^k - \sum_{k=1}^{n_e} \frac{1}{2} AE_k \sum_{z=1}^{m_d} \int_0^{l_k} \frac{\partial [S_z(\varsigma)]_k^T}{\partial \varsigma} \{d_r\}_k^T \frac{\partial [N_r(\varsigma)]_k^T}{\partial \varsigma} \times \frac{\partial [N_r(\varsigma)]_k}{\partial \varsigma} \{d_r\}^k \, d\varsigma \right\}, \tag{A.12}$$

$$
\begin{aligned}
[k]^* = \sum_{k=1}^{n_e} k_1 \sum_{r=1}^{n_d} \Bigg\{ & \left[N_r\left(v_0 t + \frac{1}{2} a_0 t^2 \right) \right]_k^{\mathrm{T}} \left[N_r\left(v_0 t + \frac{1}{2} a_0 t^2 \right) \right]_k \\
& + \sum_{k=1}^{n_e} c_1 \sum_{r=1}^{n_d} \left[N_r\left(v_0 t + \frac{1}{2} a_0 t^2 \right) \right]_k^{\mathrm{T}} \\
& \times \dot{\varsigma} \left[N_r\left(\varsigma = v_0 t + \frac{1}{2} a_0 t^2 \right) \right]_{\varsigma_k} \\
& + \sum_{k=1}^{n_e} m_2 \Bigg\{ \sum_{r=1}^{n_d} \left[N_r\left(\varsigma = v_0 t + \frac{1}{2} a_0 t^2 \right) \right]_k^{\mathrm{T}} \\
& \times (v_0 + a_0 t)^2 \left[N_r\left(\varsigma = v_0 t + \frac{1}{2} a_0 t^2 \right) \right]_{\varsigma\varsigma_k} \\
& + \left[N_r\left(\varsigma = v_0 t + \frac{1}{2} a_0 t^2 \right) \right]_{\varsigma k} a_0 \Bigg\} \Bigg\}. \qquad \text{(A.13)}
\end{aligned}
$$

References

[1] Salawu OS. Detection of structural damage through changes in frequency: a review. Eng Struct 1997;19(9): 718–23.

[2] Doebling SW, Farrar CR, Prime MB. A summary review of vibration-based damage identification methods. Shock Vibr Digest 1998;30(2):91–105.

[3] Ewins DJ. Modal testing: theory, practice and application. Baldock Hertfordshire: Research Studies Press Limited; 2000.

[4] Frisswell MI, Mottershead JE. Finite element model updating in structural dynamics. Dordrecht: Kluwer Academic Publishers; 1996.

[5] Ewins DJ. Adjustment or updating of models. In: Kundra TK, Nakra BC, editors. Proceedings of IUTAM-IITD International Winter School on Optimum Dynamic Design. New Delhi: Allied Publishers Limited; 1997.

[6] Wang D, Haldar A. Element-level system identification with unknown input. J Eng Mech, ASCE 1994;120(1):159–76.

[7] Hermans LUC, Auweraer HVD. Extraction and validation of structural models from tests under operational conditions. In: Proceedings of Symposium of International Automotive Technology. SIAT/SAE Technical Paper Series, Pune, India, 1999. p. 293–302.

[8] Doebling SW, Farrar CR, Prime MB. A summary review of vibration-based damage identification methods. Shock Vibr Digest 1998;30(2):91–105.

[9] Mazurek DF, DeWolf JT. Experimental study of bridge monitoring technique. J Struct Eng, ASCE 1990; 116(9): 2532–49.

[10] Hearn G, Testa RB. Modal analysis for damage detection in structures. J Struct Eng, ASCE 1991;117(10): 3042–63.

[11] Yao GC, Chang KC, Lee GC. Damage diagnosis of steel frames using vibrational signature analysis. J Eng Mech, ASCE 1992;118(9):1949–61.

[12] Alampalli S, Fu G. Remote monitoring systems for bridge condition. Client report 94, Transportation Research and Development Bureau, New York State Department of Transportation, 1994.

[13] Alampalli S. Significance of operating environment in condition monitoring of large civil structures. Shock Vibr 1999;6:247–51.

[14] Alampalli S, Fu G, Dillon EW. Measuring bridge vibration for detection of structural damage. Research report 165, Transportation Research and Development Bureau, New York State Department of Transportation, 1995.

[15] Alampalli S, Cioara TGH. Selective random decrement technique for processing bridge vibration data. In: Alampalli S, editor. Proceedings of Conference on Structural Materials Technology IV. Lancaster: Technomic Publishers Co.; 2000. p. 75–80.

[16] Casas JR, Aparicio AC. Structural damage detection from dynamic test data. J Struct Eng, ASCE 1994;120(8): 2437–50.

[17] Koh CG, See LM, Balendra T. Damage detection of buildings: numerical and experimental studies. J Struct Eng, ASCE 1995;121(8):1155–60.

[18] Liu PL. Identification and damage detection of trusses using modal data. J Struct Eng, ASCE 1995;121(4):599–608.

[19] Salawu OS, Williams C. Bridge assessment using forced-vibration testing. J Struct Eng, ASCE 1995;121(2):161–73.

[20] Wahab MM, Roeck GD. Dynamic testing of prestressed concrete bridges and numerical verification. J Struct Eng, ASCE 1998;3(4):159–69.

[21] Kosmatka J, Ricles JM. Damage detection in structural modal vibration characterization. J Struct Eng, ASCE 1999;125(12):1384–92.

[22] Majumder L, Manohar CS. A time domain approach for damage detection in beam structures using vibration data with a moving oscillator as an excitation source. J Sound Vibr; in press. doi:10.1016/S0022-460X(02)01555-9.

[23] Hino J, Yoshimura T, Ananthanarayana N. Vibration analysis of nonlinear beams subjected to a moving load using the finite element method. J Sound Vibr 1985;100:477–91.

[24] Yoshimura T, Hino J, Kamata T, Ananthanarayana N. Random vibration of a nonlinear beam subjected to a moving load by a finite element analysis. J Sound Vibr 1988;122:317–29.

[25] Lee U. Revisiting the moving mass problem: onset of separation between the masses and beam. Trans ASME, J Vibr Acoust 1996;118:516–21.

[26] Bathe KJ. Finite element procedures. New Jersey: Prentice-Hall; 1997.

[27] Sirovich L. Turbulence and the dynamics of coherent structures, part I: coherent structures. Quart Appl Math 1987;45:561–71.

[28] Sirovich L. Turbulence and the dynamics of coherent structures, part II: symmetries and transformations. Quart Appl Math 1987;45:573–82.

[29] Sirovich L. Turbulence and the dynamics of coherent structures, part III: dynamics and scaling. Quart Appl Math 1987;45:583–90.

[30] Berkooz G, Holmes P, Lumley JL. The proper orthogonal decomposition in the analysis of turbulent flows. Ann Reports Fluid Mech 1993;25:539–75.
[31] Newman AJ. Model reduction via the Karhunen–Loeve expansion, part I: an exposition. Technical research report, TR 96-32, Institute for Systems Research; 1996.
[32] Newman AJ. Model reduction via the Karhunen–Loeve expansion, part II: some elementary examples. Technical research report, TR 96-33. Institute of Systems Research; 1996.
[33] Noor AK. Recent advances and applications of reduction methods. Appl Mech Rev 1994;47:125–45.
[34] Matthies HG, Meyer M. Nonlinear Galerkin methods for the model reduction of nonlinear dynamical systems. Comput Struct 2003;81:1277–86.
[35] Callahan JO, Avitabile P, Riemer R. System equivalent reduction expansion process (SEREP). In: Proceedings of the 7th International Modal Analysis Conference, Las Vegas, Nevada, February 1989. p. 29–37.